



Universiteit
Leiden
The Netherlands

Size effects on atomic collapse in the dice lattice

Oriekhov, D.; Voronov, S.O.

Citation

Oriekhov, D., & Voronov, S. O. (2023). Size effects on atomic collapse in the dice lattice. *Journal Of Physics: Condensed Matter*, 36. doi:10.1088/1361-648X/ad146f

Version: Publisher's Version

License: [Creative Commons CC BY 4.0 license](https://creativecommons.org/licenses/by/4.0/)

Downloaded from: <https://hdl.handle.net/1887/4171962>

Note: To cite this publication please use the final published version (if applicable).



PAPER • OPEN ACCESS

Size effects on atomic collapse in the dice lattice

To cite this article: D O Oriekhov and S O Voronov 2024 *J. Phys.: Condens. Matter* **36** 125603

View the [article online](#) for updates and enhancements.

You may also like

- [Twisted graphene superlattices: resonating valence bond states and magnetic properties](#)
Florentino López-Urías, Alberto Rubio-Ponce, Emilio Muñoz-Sandoval et al.
- [Superfluid states in \$-T_c\$ lattice](#)
Yu-Rong Wu, , Yi-Cai Zhang et al.
- [Synthetic gauge fields for lattices with multi-orbital unit cells: routes towards a - flux dice lattice with flat bands](#)
Gunnar Möller and Nigel R Cooper

Size effects on atomic collapse in the dice lattice

D O Oriekhov^{1,*}  and S O Voronov² 

¹ Instituut-Lorentz, Universiteit Leiden, PO Box 9506, 2300 RA Leiden, The Netherlands

² National Technical University of Ukraine 'Igor Sikorsky Kyiv Polytechnic Institute', Beresteyskyi Ave. 37, 03056 Kyiv, Ukraine

E-mail: d.oriekhov@gmail.com

Received 18 September 2023, revised 30 November 2023

Accepted for publication 11 December 2023

Published 20 December 2023



CrossMark

Abstract

We study the role of size effects on atomic collapse of charged impurity in the flat band system. The tight-binding simulations are made for the dice lattice with circular quantum dot shapes. It is shown that the mixing of in-gap edge states with bound states in impurity potential leads to increasing the critical charge value. This effect, together with enhancement of gap due to spatial quantization, makes it more difficult to observe the dive-into-continuum phenomenon in small quantum dots. At the same time, we show that if in-gap states are filled, the resonant tunneling to bound state in the impurity potential might occur at much smaller charge, which demonstrates non-monotonous dependence with the size of sample lattice. In addition, we study the possibility of creating supercritical localized potential well on different sublattices, and show that it is possible only on rim sites, but not on hub site. The predicted effects are expected to naturally occur in artificial flat band lattices.

Keywords: coulomb impurity, atomic collapse, flat band, dice lattice, quantum dot

1. Introduction

The phenomenon of atomic collapse was firstly discussed in connection with Dirac equation describing electrons near super-heavy nuclei [1, 2]. If the charge of such nuclei exceeds the critical value $Z > 170$, the lowest energy state in Coulomb field reaches lower continuum and creation of electron–positron pair becomes possible [3]. With the discovery of two-dimensional materials with Dirac cones in spectrum the atomic collapse again attracted attention [4–7]. The main reason was that critical charge required for creation of electron–hole pair was estimated to be $Z_{cr}/\kappa = 1/2$ with κ being a dielectric constant. Later studies has shown that the presence of gap

induced by a gate [8] or by a spatial quantization due to finite size [4, 9], as well as polarization effects [5] make the critical charge a bit larger, slightly exceeding $Z_{cr}/\kappa \gtrsim 1$. A number of experiments [10–12] were performed in graphene to analyze the effects that appear when the charge of impurity becomes supercritical. Firstly the collapse states were observed in experiments with impurities made as clusters of atoms [10], and later the realizations as vacancy or induced by scanning tunneling microscope (STM) tip appeared [11, 12].

After these experiments appeared, a number of properties of atomic collapse states were studied. In particular, atomic collapse and formation of bound states was analyzed for graphene in external perpendicular magnetic field in [13, 14] due to effect of dimensional reduction. The much smaller critical charge values were predicted for bilayer graphene as a result of more flat dispersion of quasiparticles [15, 16]. Notably, the supercritical impurity in bilayer graphene does not lead to a collapse of wave functions in analytic description. In addition, it was predicted that atomic collapse effect may happen in another material, a donor cluster in SrTiO₃ [17] and might

* Author to whom any correspondence should be addressed.



Original Content from this work may be used under the terms of the [Creative Commons Attribution 4.0 licence](https://creativecommons.org/licenses/by/4.0/). Any further distribution of this work must maintain attribution to the author(s) and the title of the work, journal citation and DOI.

be controlled by a size of a cluster. Another way to control the critical charge is a tilt of Dirac cones in 2D materials [18]. Theoretical studies has also shown that the supercritical instability can be induced dynamically by charged ions passing through graphene samples [19].

The new generation of two-dimensional materials that host flat bands in addition to Dirac cones [20] again posed a question on which effects the Coulomb impurity will produce. In [21–23] it was shown by analytical and numerical calculations for dice lattice that the bound states decouple also from the flat band. In the case of infinite lattice model the flat band fully decomposes into a continuous spectrum in the field of Coulomb impurity because the pure Coulomb potential is long-range [21, 23]. Additional simulations on a finite lattice model with large sample size have shown that the bound states decoupled from flat band anticross with atomic collapse states coming from the upper dispersive band [24].

The present study is motivated by the experiments with electronic lattices such as Lieb [25] and honeycomb with s-p hybridization [26, 27], which might serve as potential platform to realize also the dice lattice. The artificial lattices of such kind have approximately ten times larger lattice constant than atomically-thin materials and thus much weaker electron–electron interactions. Thus, the effects of single-particle physics in external field might be easier to observe than in strongly-correlated flat band systems. In addition, one should note the typical sample size difference between atomic samples and electronic artificial lattices. The latter have a size of order of 10 sites along each side [25–27], making the role of edges significant in any studied effect. To analyze the role of size effects on the possibility of observation of atomic collapse we consider quantum dots of circular shape made of dice lattice. The shape of quantum dot and potential well might be controlled by the techniques developed in [12] with a circular p–n junctions, that is created by a deep potential well created by the tip-induced charge.

From the classification of the dice lattice terminations [28] it is known that particular boundary conditions lead to the gapless spectrum. In the case of gapped model [29, 30] the number of in-gap states is formed. In the circular shape of quantum dot all such terminations appear, thus leading to the existence of in-gap edge states. The electrons from such energy levels, if filled, may tunnel to the bound state near Coulomb impurity, leading to the atomic collapse. Such effects will screen Coulomb impurity much earlier than the actual critical charge of infinite lattice is reached. In the present paper we study how the critical charge of impurity depends on potential localization as well as modified by in-gap edge states.

A number of properties of finite size dice lattice quantum dots were studied in recent years. Among them are the description of distributions of edge currents in quantum dots [31], prediction appearance of Majorana corner states in the presence of Rashba coupling [32], size dependence of Landau levels formed in the ring made of $\alpha - T_3$ lattice [33], analysis of the role of atomic effects in narrow zigzag ribbons [34], valley filtering [35, 36] and dynamical formation of bound states by external driving [37] in $\alpha - T_3$ lattice quantum dots. The

formation of pseudo-Landau levels in nonuniform strain for triangular shaped quantum dots was discussed in [38]. As an additional tool, the polarized light with its dressing electromagnetic field can be used to create finite-sized potential wells in dice lattice, generate different type of gaps and study the transport properties [39–43]. The study of the effect of edges on atomic collapse in graphene nanoribbons was made in [44]. In addition, the role of graphene quantum dot size on atomic collapse in magnetic field was done in [45].

The paper is organized as follows: in section 2 we describe the models of quantum dots used in tight-binding simulations. In section 3 we describe the simulation technique and perform the brief analysis of atomic collapse in large quantum dots for the usual and screened Coulomb potential modeled via faster decaying coordinate dependence. In section 4 we analyze the atomic collapse for the same potentials in a small quantum wells. The presence of edge states modifies the results comparing to large systems. In addition, we study a possibility of creating supercritical impurity by localized potential well in the center of the system. Different positions of such well are analyzed in section 5. Finally, we compare all results to those obtained for large [24] and infinite systems [21, 23] in section 6 and make the conclusions about expected observable signatures of atomic collapse in experiments with small artificial lattices.

2. Quantum dots made of dice lattice

In the present paper we consider a dice lattice as a representative example of flat band model which hosts pseudospin-1 fermions. The previous extensive theoretical studies of atomic collapse in dice lattice allow one to distinguish effects that appear due to finite size from those that was characteristic to infinite model. The geometry is shown in figure 1(a). It contains three sublattices, two of which (A,B) are connected only with third one (C) by corresponding hopping parameters t_{AC} and t_{BC} . The basis vectors of underlying Bravais lattice are $\mathbf{a}_1 = (1, 0)a$ and $\mathbf{a}_2 = (1/2, \sqrt{3}/2)a$. The tight-binding equations describing this system are [46–48]:

$$\begin{aligned} \varepsilon \Psi_A(\mathbf{r}) &= m_A \Psi_A(\mathbf{r}) - t_{AC} \sum_j \Psi_C(\mathbf{r} + \delta_j), \\ \varepsilon \Psi_B(\mathbf{r}) &= m_B \Psi_B(\mathbf{r}) - t_{BC} \sum_j \Psi_C(\mathbf{r} + \delta_j), \\ \varepsilon \Psi_C(\mathbf{r}) &= m_C \Psi_C(\mathbf{r}) - t_{AC} \sum_j \Psi_A(\mathbf{r} + \delta_j) \\ &\quad - t_{BC} \sum_j \Psi_B(\mathbf{r} - \delta_j). \end{aligned} \quad (1)$$

Here the vectors δ_j connect neighboring A atoms with C atom and are defined as [28] $\delta_1 = \frac{\mathbf{a}_1 + \mathbf{a}_2}{3}$, $\delta_2 = \frac{\mathbf{a}_3 + \mathbf{a}_1}{3}$, $\delta_3 = \frac{\mathbf{a}_2 + \mathbf{a}_3}{3}$ with $\mathbf{a}_3 = \mathbf{a}_2 - \mathbf{a}_1$. Below we use the equal hopping parameters $t_{AC} = t_{BC} = t$ that correspond to the dice model. It is possible to open a gap in spectrum and separate the flat band from others by adding onsite potentials of opposite signs to A and B sublattices: $m_A = -m_B = m$ and $m_C = 0$. Below we

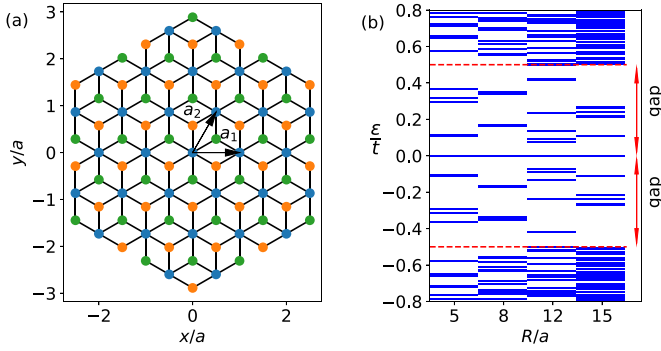


Figure 1. (a) Schematic plot of the dice lattice for quantum dot of radius $R = 3a$. The spectrum of quantum dot appearing for several values of radius are shown in (b) for gap parameter $m = 0.5t$. The appearance of in-gap edge states is marked by arrows on the right, that denote gapped regions of the bulk. For the small quantum dot sizes ($R = 5a$ and $R = 8a$ in the plot) the extension of a spectral gap coming from size quantization is clearly visible.

select $m = 0.5t$ as a values of mass parameter for all calculations. Such selection of mass term out of many discussed in the literature [21, 24, 39, 48, 49] is motivated by the possibility of separating flat band from others and clear way of realizing the band gap in experiment by applying the same onsite potential with alternating sign. In addition, such band gap keeps the structure of the spectrum similar to what is obtained for different insulator-type boundary conditions [28, 29]. The spectrum of such model consists of three bands separated by gaps, which have the following dispersion in k-space:

$$\varepsilon_{\pm}(\mathbf{k}) = \pm \sqrt{m^2 + 2|f(\mathbf{k})|^2}, \quad \varepsilon_0 = 0, \\ f(\mathbf{k}) = -t(1 + e^{-i\mathbf{k}a_2} + e^{-i\mathbf{k}a_3}). \quad (2)$$

In addition, one should expect the appearance of in-gap edge states that would be specific for the type of lattice termination chosen. The examples of spectrum for several sizes of circular quantum dot are shown in panel (b) of figure 1. The atomic collapse in the infinite lattice with such gap term was studied in [21, 23]. The presence of gap term in spectrum allows one to distinguish the level repulsion related to the atomic collapse in the bulk of sample from the mixing with in-gap edge states that makes the state less localized. In addition, the mixing with edge states becomes suppressed as the gap term enforces their localization closer to the boundaries, thus leading to smaller overlap with bound state near impurity.

2.1. Description of model potentials and tight-binding simulations

The approach used in the simulations is similar to that described in [24, 44] and the code for all presented results can be found at [50]. We start with the lattice model of quantum dot implement with the help of Kwant code [51]. The spectrum of finite size system contains all levels coming from bulk and edge states. They evolve differently with growing charge of impurity, in particular the far-away placed edge states stay

nearly at the same energy. In order to avoid complicated procedures of distinguishing atomic collapse states from such edge states, we calculate a energy-resolved local density of states (LDOS) in the central unit cell of the quantum dot. The calculation is performed by using kernel polynomial method with a high number of moments (typically of the order of 10^4) that ensures precise energy resolution of the plots [52]. The calculation of LDOS also guarantees that the shown states are only those that contribute into physics in the vicinity of impurity and are possible to measure via STM-type techniques.

The model potentials used to describe a normal and screened Coulomb impurity made as adatom on top of the lattice are:

$$V(\mathbf{r}) = -V \frac{a^n}{(|\mathbf{r}|^2 + r_0^2)^{n/2}}. \quad (3)$$

Here r_0 is the regularization radius of impurity and $n = 1$ corresponds to the pure Coulomb potential. Below in the numerical calculations we fix the depth of potentials with different n to be the same at $\mathbf{r} = 0$. This is done by setting $r_0 = a$ for all potentials. Another choice would be to set different r_0 depending on powers n and keep the constant $(a/r_0)^n$ the same. That would result in effective normalization of V parameter and produce qualitatively the same results. As a motivation for such model of long- and short-range potentials we note that the $n = 3$ power case describes the Coulomb impurity with dynamical one-loop polarization screening in monolayer graphene [53]. The comparison of bound state picture that decouple from flat band in such potentials in a lattice model would highlight the effect of localized structure of a flat band states. Indeed, to prove that flat band decomposes into continuum-type spectrum in Coulomb potential, a special convergence-checking technique was used in effective low-energy model [23]. Below we show that lattice calculations support that conclusion with correction to finite state number in the system, while the short-range potentials demonstrate different behavior.

3. Atomic collapse in Coulomb and power-law potentials

In this section we analyze how the bound states evolve with potential strength V of impurity for a large system size. Specifically, we take the quantum dot of radius $R = 50a$ centered at C atom and place impurity at the center of a disk. The results of simulation are shown in figure 2 for powers $n = 1$ to $n = 4$ of model potential (3). The results presented in this section for a Coulomb potential are in agreement with results of [24]. In addition we tested the parameters of [24] to check the convergence of the simulations. In the next section we analyze the smaller system sizes to uncover effects of edge states on atomic collapse in quantum dots.

Before proceeding to the description of main results, let us briefly recall the description of long-studied phenomena of atomic collapse in relativistic systems. Mathematically it appears that in a pure Coulomb potential the energy of a first

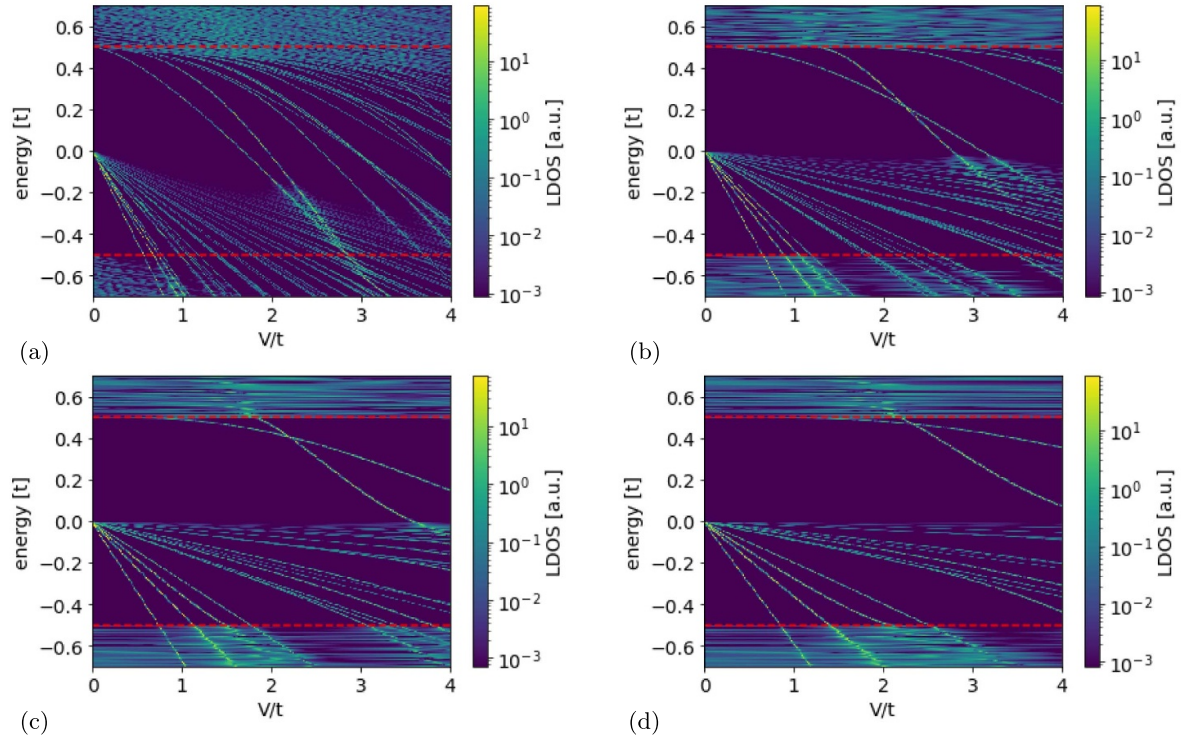


Figure 2. LDOS in central unit cell as a function of potential strength for power $n = 1, 2$ upper row and $n = 3, 4$ lower row. Quantum dot size is $R = 50a$. Regularization radius was taken $r_0 = a$. The gap size is $m = 0.5t$. The (a) $n = 1$ power corresponds to bare Coulomb potential and demonstrates the largest density of bound states decoupled from flat band.

bound state of relativistic particle has a form of [1, 2] $\varepsilon = m\sqrt{1 - (\alpha Z)^2}$, with α being a fine structure constant. Such energy becomes imaginary after critical charge value $Z > 1/\alpha$, manifesting the instability of a ground state [1, 2, 6, 7]. In the regularized potential the mathematical ‘collapse’ is replaced by a dive-into-continuum phenomena, where the lowest bound state reaches the lower conducting band and the electrons tunnel from there, creating a hole that moves away from charge impurity [8]. Such tunneling results in an effective screening of impurity by electron filling a bound state, reducing its charge by one. Below in all tight-binding simulations we analyze the presence and properties of dive-into-continuum phenomena in small-sized lattices. The detailed structure of the bound states for near-critical charges of impurity was studied for very large dice lattice ribbons in [24].

From the spectral plots shown in figure 2 the following conclusions can be made: the critical charge for the first bound state decoupled from the upper band is larger than for the second only for Coulomb potential with $n = 1$. For the infinite system such structure in spectrum appeared for states with angular momentum $j = 0$ and $j = 1$ with $j = 1$ firstly decoupling from continuum [21]. For the large system size the in-gap states do not influence atomic collapse happening in the bulk.

For the flat band the density of bound states that decouple at small charges becomes lower with increasing power of potential n . The energy separation of such states also becomes larger with n . This agrees with the prediction of [21, 23] that flat band decomposes into continuum of states in the long-range potential, but only a discrete set of bound states decouples in

short-range potential. The localized structure of flat band states leads to approximately linear behavior with growing charge parameter of impurity V . The slope is defined by the distance from the localization point to the potential center.

4. Atomic collapse in small quantum dots: the role of edge states

In this section we perform the simulations for much smaller system sizes where the edge states contribute to the LDOS at the central unit cell. As was shown in figure 1, the possible energies of in-gap edge states strongly depend on the size. We analyze a set of different radius values to describe the qualitative role of edge states on critical charge value. One should note that to obtain precise numerical values a simulation should be made for a sample geometry available in experiment. However, a number of conclusions can be made from analysis of a set of different samples.

Firstly we present the results of calculations for the system with radius $R = 10a$, that are shown in figure 3 for the powers $n = 1$ to $n = 4$ of model potential (3). Due to the small size of the system all levels in spectrum decrease in energy with increasing charge of impurity. The in-gap edge states demonstrate nearly linear dependence of energy on potential strength V , which follows from their localization and nearly zero kinetic energy. But, the resonant anticrossing of bound states decoupled from the bands with such in-gap states lead to

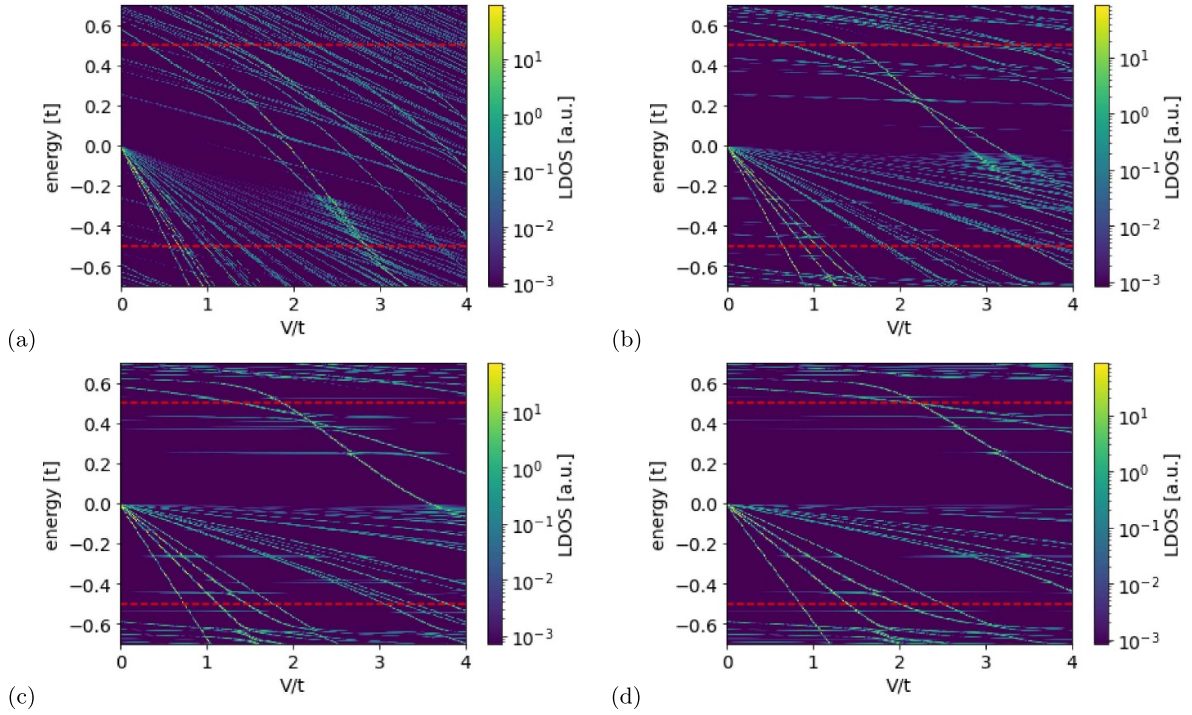


Figure 3. LDOS in central unit cell as a function of potential strength for $n = 1, 2$ upper row and $n = 3, 4$ lower row. Disk size is $R = 10a$. Note that these results are for intermediate disk size, which would describe the artificial lattices made of a set of individual sites (atoms or clusters). Regularization radius was taken $r_0 = 1a$. The gap size is $m = 0.5t$. A number of level repulsions with in-gap edge states are clearly visible in all plots. Several edge states also decrease in energy in a bare Coulomb potential in panel (a).

the appearance of nontrivial dependence on V for both. In addition, such anticrossings modify the value of critical charge for the dive-into-continuum type problem. We define such charge as the position of the first intersection between levels originating from different bands in infinite model (e.g. upper band levels to flat band, and flat-to-lower band). In the case when in-gap states are filled, one may expect much lower values of critical charge required to screen the impurity by electron tunneled to bound state.

4.1. Size effect on a critical charge value

Next we analyze the role of radius of quantum dot on the critical charge values as well as first level repulsion with in-gap state in Coulomb potential. The figure 4 shows results for the levels decoupled from upper band in panel (a) and from the flat band in panel (b). Both plots show that the critical charge for dive-into-continuum charge grows with decreasing radius of quantum dot. The first effect that should be taken into account for understanding these results is a gap size growing due to the spatial discretization of momentum. Taking the dispersion (2) and linearizing near one of the K -points, one finds

$$\varepsilon_+ = \sqrt{m^2 + v_F^2 k^2}, \quad v_F = \sqrt{3}ta/2. \quad (4)$$

The uncertainty relation leads to the minimal value of momentum $k \sim 1/R$, that leads to the following increase of the gap value

$$\delta_m \sim \frac{t^2}{m} \left(\frac{\sqrt{3}a}{2R} \right)^2, \quad (5)$$

where we used series expansion of (4). In addition to such increase of gap, two other effects play a role. As was discussed above, in small-scale finite system all levels decrease in energy in external long-range potential. Consequently, the first levels of lower continuum appear below effective gap energy when potential strength is nonzero, making the required V_{crit} slightly larger. In addition, the nontrivial role is played by the presence of one or several resonant anti-crossings with in-gap edge states, that result in a change of the critical charge value. Such anti-crossings are a result of finite overlap between bound state and in-gap edge state wave functions. This overlap leads to an existence of two eigenstates of a Hamiltonian of the system nearly at the same energy, that have a form of superposition of bound state and edge state wave functions. To separate the bound state back from superposition a further increase of potential is needed. These are the main qualitative reasons on why for the flat band we observe non-monotonous behavior of dive-into-continuum V_{crit} values.

5. Supercritical localized potential well

In this section we analyze the possibility of forming the dive-into-continuum bound states by a localized potential well. As an example of experimental implementation one can consider setup from [12] where the atomic collapse in graphene was

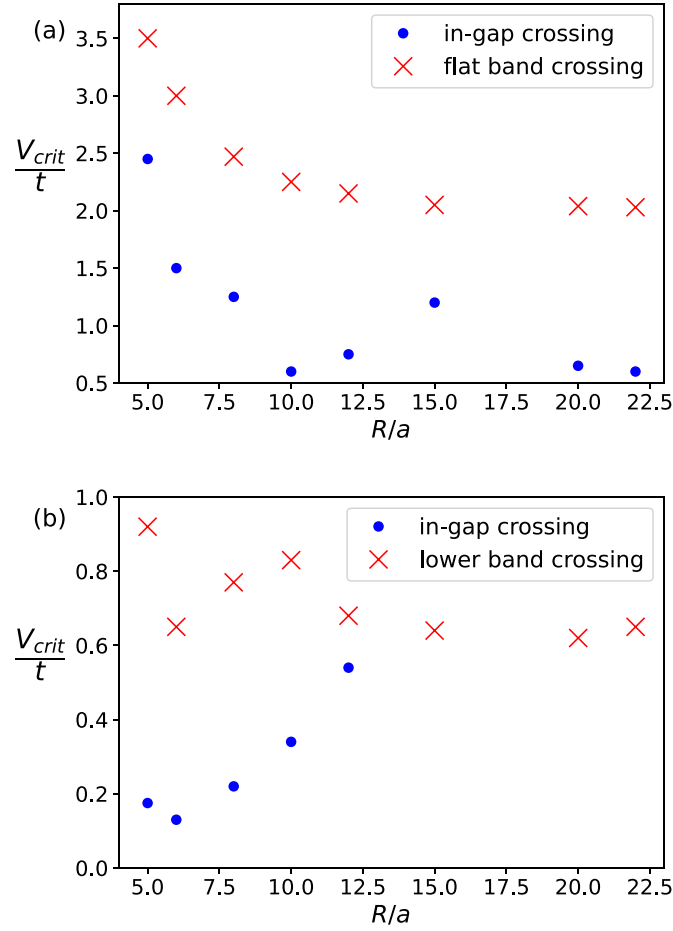


Figure 4. Size dependence of potential values at which the first repulsion with bound in-gap state happens and when the dive-into-continuum phenomenon between states originating from different bands is happening. Panel (a) shows the results for states originating from upper band, and panel (b) for the states from flat band.

observed in potential well of circular p–n junction. We investigate the potential wells that are centered at single sublattice. Other potential wells that cover several sites are very close to model potentials (3) with large n (already $n = 4$ is close to localized potential well) and would not lead to qualitatively new results.

The results of calculation of LDOS are presented in upper row of figure 5. The localized potential well decouples bound states from the flat band much earlier than from upper band. In the plots shown in figure 5 we focus on the evolution of energy for such bound states with increasing charge. Only single state is decoupled as there is only single state in flat band localized exactly at the position of potential well. Notably, for the C -localized potential well the bound state approaches the lower band asymptotically with growing V . Also this bound state has the largest value of occurred level repulsions inside the gap, which leads to the largest delocalization of its wave function.

The lower row in figure 5 shows the distribution of wave function for a bound state at such values of potential that the energy level is placed inside the gap. For all cases the distribution shows C_3 -symmetric pattern keeping the discrete symmetry of the lattice. The notable difference between A -, B -localized and C -localized potential wells is that in the first two

cases the highest density is placed exactly at potential well site. Instead, for the C -localized well the maximum density values are distributed symmetrically around C site. The state itself is not as localized as two other examples, and has a small density at the site with potential. Indeed, by calculating density $|\Psi_C(\mathbf{r} = 0)|^2$ at central C atom with potential well for different values of V , we find that it decreases with growing V (see figure 6). As was shown in [21], the C -component of a wave function in a free continuum model is given by the middle component of a momentum k dependent spinor

$$\psi_{\pm,0}(\mathbf{k}) = N^{-1}(\mathbf{k}) \begin{pmatrix} \frac{(m+\varepsilon_{\pm,0})}{\sqrt{2}}(k_x - ik_y) \\ \varepsilon_{\pm,0}^2 - m^2 \\ -\frac{(m-\varepsilon_{\pm,0})}{\sqrt{2}}(k_x + ik_y) \end{pmatrix}, \quad (6)$$

where N is a normalization constant. It behaves as $\Psi_C \sim (\varepsilon^2 - m^2)$, tending to zero when $\varepsilon \rightarrow \pm m$. Such dependence on energy compensates the potential strength and leads to asymptotic approaching of lower band by a bound state (see figure 5(c)). The small dip at $V = 8t$ in figure 6 is related to the repulsion with in-gap energy level and does not affect the general qualitative picture.

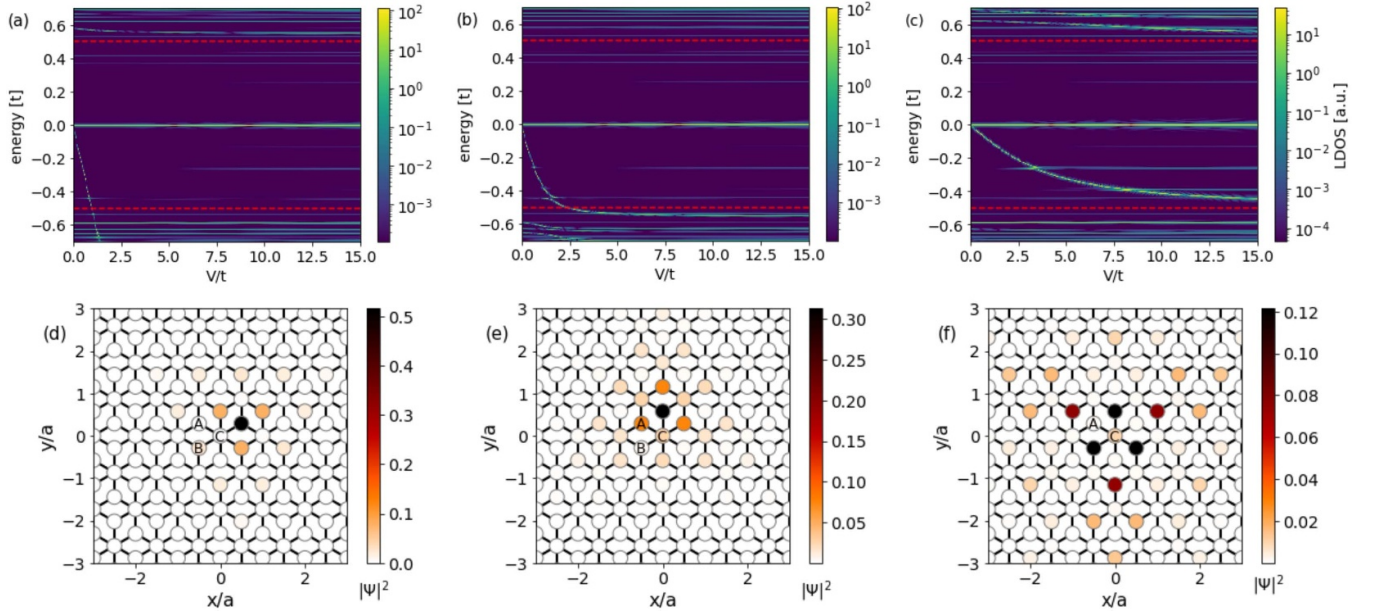


Figure 5. Upper row: LDOS in central unit cell as a function of potential strength for potential well localized at single site (a) A, (b) B and (c) C respectively. Quantum dot size is $R = 10a$ and the gap size is $m = 0.5t$. The bound state for C-localized well asymptotically reaches the lower continuum. Lower row: wave function distribution for a bound state at potential values (d), (e) $V = 0.6t$, and (f) $V = 10t$ with localizations at A, B and C corresponding to upper row.

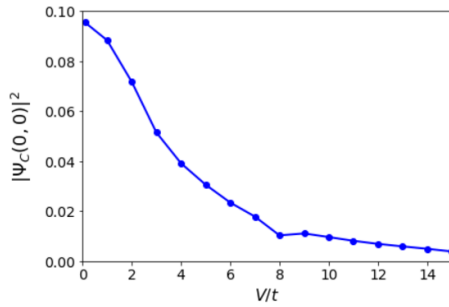


Figure 6. Dependence of C-component of wave function density $|\Psi_C(\mathbf{r}=0)|^2$ on the central atom for the potential well localized at C-atom. The decreasing value of wave function compensates the growing potential value, leading to the asymptotic approaching of the lower continuum by a bound state decoupled from a flat band.

In addition, we note that the bound states decoupled from the flat band for the A- and B-localized potential demonstrate near linear behavior of energy dependence with growing potential. The level repulsion with in-gap state for B-localized quantum well leads to the larger critical charge. The asymmetry between A- and B-localized well cases appears due to the gap that takes $+m$ value at A site and $-m$ at B site, while potential has the same sign $-V$.

6. Conclusions

In the present paper we analyzed the role of size effect on the possibility of observing atomic collapse phenomenon in the quantum dots made of dice lattice. Depending on whether in-gap edge states are filled, the critical charge takes different

values for the same system size. The size dependence itself of critical charge for dive-into-continuum problem demonstrates non-monotonous behavior due to a number of level-repulsion events happening with the bound state inside the gap. These level repulsions in spectrum show the appearance of superposition-type states, localized partially on the interior of the system, where the potential is weak. That makes the effect of potential weaker and requires larger charge to put bound state energy below the gap value.

In addition to the size effect happening due to finite radius of quantum dot, we analyzed the role of the effective range of potential in decoupling bound states from flat band. It is shown that while the long-range potential decomposes flat band into a dense set of bound states, more short-range potentials result in large gap separations between lowest bound states. Such effects might occur when the Coulomb impurity is dynamically screened. In addition, this result supports the conclusion about full decomposition of a flat band by long-range potential, found earlier in a continuum model by solving problem exactly at zero energy [21] and showing the convergence to continuum spectrum of bound states numerically [23].

Next we analyzed the possibility of creating supercritical localized potential well on a single site. The structure of wave functions in the dice model allows the formation of bound state decoupled from the flat band, but makes the threshold potential very large for the decoupling of bound state from the upper band. The dive-into-continuum situation occurs only to rim-placed potential wells, but not for hub-centered. This can be explained by the fact that wave functions has zero hub component exactly at the gap edge, thus making it impossible to cross by a bound state localized only on a hub site. In conclusion we note that these results describe the potential

possibility of finding atomic collapse in artificial electronic flat band lattices, where the single-particle physics might be easier to study due to the larger lattice constant [25] and weaker electron-electron interactions.

Data availability statement

All data that support the findings of this study are included within the article (and any supplementary files).

Acknowledgments

We are grateful to E V Gorbar and V P Gusynin for fruitful discussions. D O O acknowledges the support from the Netherlands Organization for Scientific Research (NWO/OCW) and from the European Research Council (ERC) under the European Union's Horizon 2020 research and innovation program.

ORCID iDs

D O Oriekhov  <https://orcid.org/0000-0002-1976-0937>

S O Voronov  <https://orcid.org/0000-0002-0053-0381>

References

- [1] Pomeranchuk I Y and Smorodinsky Y A 1945 On the energy levels of systems with $Z > 137$ *J. Phys. USSR* **9** 97
- [2] Zeldovich Y B and Popov V S 1972 Electronic structure of superheavy atoms *Sov. Phys. - Usp.* **14** 673
- [3] Greiner W, Muller B and Rafelski J 1985 *Quantum Electrodynamics of Strong Fields* (Springer)
- [4] Pereira V M, Nilsson J and Neto A H C 2007 Coulomb impurity problem in graphene *Phys. Rev. Lett.* **99** 166802
- [5] Fogler M M, Novikov D S and Shklovskii B I 2007 Screening of a hypercritical charge in graphene *Phys. Rev. B* **76** 233402
- [6] Shytov A V, Katsnelson M I and Levitov L S 2007 Vacuum polarization and screening of supercritical impurities in graphene *Phys. Rev. Lett.* **99** 236801
- [7] Shytov A V, Katsnelson M I and Levitov L S 2007 Atomic collapse and quasi-rydberg states in graphene *Phys. Rev. Lett.* **99** 246802
- [8] Gamayun O V, Gorbar E V and Gusynin V P 2009 Supercritical Coulomb center and excitonic instability in graphene *Phys. Rev. B* **80** 165429
- [9] Pereira V M, Kotov V N and Neto A H C 2008 Supercritical Coulomb impurities in gapped graphene *Phys. Rev. B* **78** 085101
- [10] Wang Y *et al* 2013 Observing atomic collapse resonances in artificial nuclei on graphene *Science* **340** 734
- [11] Mao J, Jiang Y, Moldovan D, Li G, Watanabe K, Taniguchi T, Masir M R, Peeters F M and Andrei E Y 2016 Realization of a tunable artificial atom at a supercritically charged vacancy in graphene *Nat. Phys.* **12** 545
- [12] Jiang Y, Mao J, Moldovan D, Masir M R, Li G, Watanabe K, Taniguchi T, Peeters F M and Andrei E Y 2017 Tuning a circular p-n junction in graphene from quantum confinement to optical guiding *Nat. Nanotechnol.* **12** 1045
- [13] Gamayun O V, Gorbar E V and Gusynin V P 2011 Magnetic field driven instability of a charged center in graphene *Phys. Rev. B* **83** 235104
- [14] Sobol O O, Pyatkovskiy P K, Gorbar E V and Gusynin V P 2016 Screening of a charged impurity in graphene in a magnetic field *Phys. Rev. B* **94** 115409
- [15] Oriekhov D O, Sobol O O, Gorbar E V and Gusynin V P 2017 Coulomb center instability in bilayer graphene *Phys. Rev. B* **96** 165403
- [16] Gorbar E V, Gusynin V P and Sobol O O 2018 Electron states in the field of charged impurities in two-dimensional Dirac systems *Low Temp. Phys.* **44** 371
- [17] Fu H, Reich K V and Shklovskii B I 2015 Collapse of electrons to a donor cluster in SrTiO_3 *Phys. Rev. B* **92** 035204
- [18] Fu W, Ke S-S, Lu M-X and Lü H-F 2021 Coulomb bound states and atomic collapse in tilted Dirac materials *Physica E* **134** 114841
- [19] Fillion-Gourdeau F M C, Levesque P and MacLean S 2020 Plunging in the Dirac sea using graphene quantum dots *Phys. Rev. Res.* **2** 033472
- [20] Bradlyn B, Cano J, Wang Z, Vergniory M G, Felser C, Cava R J and Bernevig B A 2016 Beyond Dirac and Weyl fermions: unconventional quasiparticles in conventional crystals *Science* **353** aaf5037
- [21] Gorbar E V, Gusynin V P and Oriekhov D O 2019 Electron states for gapped pseudospin-1 fermions in the field of a charged impurity *Phys. Rev. B* **99** 155124
- [22] Han C-D, Xu H-Y, Huang D and Lai Y-C 2019 Atomic collapse in pseudospin-1 systems *Phys. Rev. B* **99** 245413
- [23] Pottelberge R V 2020 Comment on Electron states for gapped pseudospin-1 fermions in the field of a charged impurity *Phys. Rev. B* **101** 197102
- [24] Wang J, Van Pottelberge R, Zhao W-S and Peeters F M C M 2022 Coulomb impurity on a Dice lattice: atomic collapse and bound states *Phys. Rev. B* **105** 035427
- [25] Slot M R, Gardenier T S, Jacobse P H, van Miert G C P, Kempkes S N, Zevenhuizen S J M, Smith C M, Vanmaekelbergh D and Swart I 2017 Experimental realization and characterization of an electronic Lieb lattice *Nat. Phys.* **13** 672
- [26] van den Broeke J J, Swart I, Smith C M and Vanmaekelbergh D 2021 Effective spin-orbit gaps in the *s* and *p* orbital bands of an artificial honeycomb lattice *Phys. Rev. Mater.* **5** 116001
- [27] Freeney S E, Slot M R, Gardenier T S, Swart I and Vanmaekelbergh D 2022 Electronic quantum materials simulated with artificial model lattices *ACS Nanosci. Au* **2** 198
- [28] Oriekhov D O, Gorbar E V and Gusynin V P 2018 Electronic states of pseudospin-1 fermions in dice lattice ribbon *Low Temp. Phys.* **44** 1313
- [29] Dey B, Kapri P, Pal O and Ghosh T K 2020 Unconventional phases in Haldane model of dice lattice *Phys. Rev. B* **101** 235406
- [30] Hao L 2022 Zigzag dice lattice ribbons: distinct edge morphologies and structure-spectrum correspondences *Phys. Rev. Mater.* **6** 034002
- [31] Soni R, Kaushal N, Okamoto S and Dagotto E 2020 Flat bands and ferrimagnetic order in electronically correlated dice-lattice ribbons *Phys. Rev. B* **102** 045105
- [32] Mohanta N, Soni R, Okamoto S and Dagotto E 2022 Majorana corner states in the dice lattice (arXiv:2210.09610)
- [33] Islam M, Biswas T and Basu S 2023 Role of magnetic field on the electronic properties of an α - T_3 ring (arXiv:2304.08830)
- [34] Hao L 2023 One-dimensional flat bands and Dirac cones in narrow zigzag dice lattice ribbons *Mater. Sci. Eng. B* **293** 116486
- [35] Filusch A, Bishop A R, Saxena A, Wellein G and Fehske H 2021 Valley filtering in strain-induced α - T_3 quantum dots *Phys. Rev. B* **103** 165114

- [36] Filusch A and Fehske H 2022 Tunable valley filtering in dynamically strained α - T_3 lattices *Phys. Rev. B* **106** 245106
- [37] Filusch A and Fehske H 2020 Electronic properties of α - T_3 quantum dots in magnetic fields *Eur. Phys. J. B* **93** 169
- [38] Sun J, Liu T, Du Y and Guo H 2022 Strain-induced pseudo magnetic field in the α - T_3 lattice *Phys. Rev. B* **106** 155417
- [39] Dey B and Ghosh T K 2019 Floquet topological phase transition in the α - T_3 lattice *Phys. Rev. B* **99** 205429
- [40] Dey B and Ghosh T K 2018 Photoinduced valley and electron-hole symmetry breaking in α - T_3 lattice: the role of a variable Berry phase *Phys. Rev. B* **98** 075422
- [41] Iurov A, Gumbs G, Huang D, for High Technology Materials C and of New Mexico U 2019 Peculiar electronic states, symmetries and Berry phases in irradiated α - T_3 materials *Phys. Rev. B* **99** 205135
- [42] Iurov A, Zhemchuzhna L, Fekete P, Gumbs G and Huang D 2020 Klein tunneling of optically tunable Dirac particles with elliptical dispersions *Phys. Rev. Res.* **2** 043245
- [43] Iurov A, Zhemchuzhna L, Gumbs G, Huang D and Fekete P 2022 Optically modulated tunneling current of dressed electrons in graphene and a dice lattice *Phys. Rev. B* **105** 115309
- [44] Wang J, Van Pottelberge R, Jacobs A, Van Duppen B and Peeters F M 2021 Confinement and edge effects on atomic collapse in graphene nanoribbons *Phys. Rev. B* **103** 035426
- [45] Eren I and Güçlü A 2022 Atomic collapse in graphene quantum dots in a magnetic field *Solid State Commun.* **351** 114763
- [46] Bercioux D, Urban D F, Grabert H and Häusler W 2009 Massless Dirac-Weyl fermions in a T_3 optical lattice *Phys. Rev. A* **80** 063603
- [47] Raoux A, Morigi M, Fuchs J-N, Piéchon F and Montambaux G 2014 From dia- to paramagnetic orbital susceptibility of massless fermions *Phys. Rev. Lett.* **112** 026402
- [48] Piéchon F, Fuchs J-N, Raoux A and Montambaux G 2015 Tunable orbital susceptibility in α - T_3 tight-binding models *J. Phys.: Conf. Ser.* **603** 012001
- [49] Gorbar E V, Gusynin V P and Oriekhov D O 2021 Gap generation and flat band catalysis in dice model with local interaction *Phys. Rev. B* **103** 155155
- [50] Oriekhov D O and Voronov S O 2023 Code for dice lattice tight-binding calculations presented in the manuscript (<https://doi.org/10.5281/zenodo.10223524>)
- [51] Groth C W, Wimmer M, Akhmerov A R and Waintal X 2014 Kwant: a software package for quantum transport *New J. Phys.* **16** 063065
- [52] Weiße A, Wellein G, Alvermann A and Fehske H 2006 The kernel polynomial method *Rev. Mod. Phys.* **78** 275
- [53] Katsnelson M I 2006 Nonlinear screening of charge impurities in graphene *Phys. Rev. B* **74** 201401(R)